ISSN 1062-8738, Bulletin of the Russian Academy of Sciences. Physics, 2014, Vol. 78, No. 1, pp. 43–48. © Allerton Press, Inc., 2014.
Original Russian Text © A.I. Musorin, P.V. Perepelkin, M.I. Sharipova, A.V. Chetvertukhin, T.V. Dolgova, A.A. Fedyanin, 2014, published in Izvestiya Rossiiskoi Akademii Nauk. Seriya Fizicheskaya, 2014, Vol. 78, No. 1, pp. 72–77.

Polarization-Sensitive Correlation Spectroscopy of Faraday-Effect Femtosecond Dynamics

A. I. Musorin, P. V. Perepelkin, M. I. Sharipova, A. V. Chetvertukhin, T. V. Dolgova, and A. A. Fedyanin

Faculty of Physics, Lomonosov Moscow State University, Moscow, 119991 Russia
e-mail: musorin@nanolab.phys.msu.ru

Abstract—Femtosecond dynamics of the Faraday effect is experimentally studied in thin magnetic films by polarization-sensitive correlation spectroscopy.

DOI: 10.3103/S1062873814010122

INTRODUCTION

Over the last decade a great amount of studies has been made in the area of ultrafast processes in magnetic materials by using femtosecond lasers. This area has become one of the most rapidly developing fields in the physics of magnetism due to the number of important fundamental problems and the potential for developing practical applications, particularly faster and more compact magnetic data recording, without being limited by the optical range. Another promising area is magneto-optical enhancement in, e.g., photonic crystals. Because of the structural dispersion of materials, a number of different optical effects has been observed in photonic crystals: giant optical dispersion and anomalous group velocity, frozen light, the suppression of spontaneous emissions of atoms [1–3], etc. Nonlinear magneto-optical diffraction, nonlinear magneto-optical Kerr effects in second and third optical harmonics, enhancement of the Faraday effect, and the magneto-optical Kerr effect have been studied in magnetophotonic crystals and microcavities [4–6]. The Faraday effect can be enhanced considerably by means of multiple interference, since the effect is nonreciprocal and is accumulated during multiple passes through a medium. In addition, active studies are being conducted to find new technologies that use light as an information carrier, giving us total control over its propagation in optical devices. Using magneto-optical effects one can govern the propagation of light in multilayer structures [7, 8].

Femtosecond laser pulses are widely used in studies of a variety of magnetic phenomena [9–12]. The interaction between subpicosecond pulses and magnetic materials enables us to study ultrafast changes in magnetization, spin re-orientation in a medium, and the precession of magnetic moments. Pulses of ultrashort duration allow experimental studies of ultrafast magnetic phase transitions between states. The use of femtosecond lasers also lets us control magnetic order and perform the ultrafast demagnetization of a medium. Ultrafast changes in magnetization are detected through their magneto-optical effects [13].

Besides changing the magnetization of the medium, the amplitude and phase modulation in space and time of an ultrashort pulse electric field can be achieved in multilayer structures upon the coherent composition of transmitted and rereflected waves. Thin magnetic films with high refractive indices are the simplest example of such structures. The time dependence of the Faraday rotation of radiation during a single femtosecond pulse (i.e., the dynamics of the Faraday effect) can be observed in these films due to multiple interference [14]. If the duration of a short light pulse is comparable to the length of a pulse transmitted through a structure, then the stationary value of Faraday rotation can not be settled, so its value changes for a period of one pulse duration. Faraday effect can differ considerably at the rising and falling edges of the pulse. Hence, experimental detection of the femtosecond dynamics of the Faraday effect related to the multiple interference of a short laser pulse in cavity structures is of great interest. The aim of this work is to investigate the femtosecond dynamics of the Faraday effect in a thin magnetic film.

MEASUREMENT TECHNIQUE

The ultrafast dynamics of the Faraday effect was studied using a polarization-sensitive technique with femtosecond time resolution. A photoelastic modulator was used in experiments to analyze the polarization state, allowing us to considerably improve the accuracy of measurement [15].

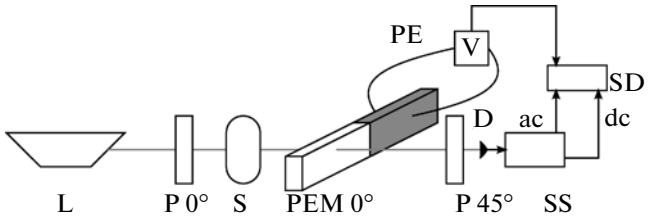

Fig. 1. Scheme for measuring stationary Faraday rotation. L, laser; P, polarizer; S, sample; PEM, photoelstic modulator; SS, signal splitter; SD, synchronous detector; PE, piezo element; D, diode.

The scheme of the experimental setup for measuring Faraday rotation using a photoelastic modulator as analyzer is presented in Fig. 1. The optical axes of the photoelastic modulator and the first polarizer are set in parallel. With this configuration, there is no alternating component at the multiple frequencies of the photoelastic modulator without a sample. If the sample is inserted into the scheme, it causes the rotation of the transmitted light's polarization plane and the detector records a signal that is proportional to the polarization plane's angle at the double frequency of the modulator.

It is convenient to calculate the analyzed polarization state using the formalism of the Mueller matrix. Let radiation, whose Stoke's vector is S_0, be incident on a Glan prism set at an angle of 0° and transmitting only horizontal polarization:

$$S_0 = \begin{pmatrix} 1 \\ 1 \\ 0 \\ 0 \end{pmatrix}.$$

The Mueller matrix for such a polarizer can be written as

$$M_1 = \frac{1}{2}\begin{pmatrix} 1 & 1 & 0 & 0 \\ 1 & 1 & 0 & 0 \\ 0 & 0 & 0 & 0 \\ 0 & 0 & 0 & 0 \end{pmatrix}.$$

After passing through the Glan prism, the M_1 vector of the state of polarization S_0 is

$$S_1 = M_1 S_0 = \frac{1}{2}\begin{pmatrix} 1 & 1 & 0 & 0 \\ 1 & 1 & 0 & 0 \\ 0 & 0 & 0 & 0 \\ 0 & 0 & 0 & 0 \end{pmatrix}\begin{pmatrix} 1 \\ 1 \\ 0 \\ 0 \end{pmatrix} = \begin{pmatrix} 1 \\ 1 \\ 0 \\ 0 \end{pmatrix}.$$

A transparent magnetized sample next to the polarizer rotates the plane of polarization by angle θ. Its Mueller matrix is

$$M_2 = \begin{pmatrix} 1 & 0 & 0 & 0 \\ 0 & \cos 2\theta & \sin 2\theta & 0 \\ 0 & -\sin 2\theta & \cos 2\theta & 0 \\ 0 & 0 & 0 & 1 \end{pmatrix}.$$

Behind the sample, the polarization vector takes the form

$$S_2 = M_2 S_1 = \begin{pmatrix} 1 & 0 & 0 & 0 \\ 0 & \cos 2\theta & \sin 2\theta & 0 \\ 0 & -\sin 2\theta & \cos 2\theta & 0 \\ 0 & 0 & 0 & 1 \end{pmatrix}\begin{pmatrix} 1 \\ 1 \\ 0 \\ 0 \end{pmatrix}$$

$$= \begin{pmatrix} 1 \\ \cos 2\theta \\ -\sin 2\theta \\ 0 \end{pmatrix}.$$

The radiation then propagates through a photoelastic modulator, which set parallel to the polarizer, Mueller matrix of the modulator is

$$M_3 = \begin{pmatrix} 1 & 0 & 0 & 0 \\ 0 & 1 & 0 & 0 \\ 0 & 0 & \cos A & -\sin A \\ 0 & 0 & -\sin A & \cos A \end{pmatrix}.$$

Here, $A = A(t) = A_0 \sin(2\pi ft)$ is a time-dependent delay introduced by the modulator, A_0 is the maximum delay of the photoelastic modulator in radians, and f is the modulation frequency. The radiation polarization vector of a light passed through the modulator is

$$S_3 = M_3 S_2 = \begin{pmatrix} 1 & 0 & 0 & 0 \\ 0 & 1 & 0 & 0 \\ 0 & 0 & \cos A & -\sin A \\ 0 & 0 & -\sin A & \cos A \end{pmatrix}$$

$$\times \begin{pmatrix} 1 \\ \cos 2\theta \\ -\sin 2\theta \\ 0 \end{pmatrix} = \begin{pmatrix} 1 \\ \cos 2\theta \\ -\sin 2\theta \cos A \\ \sin 2\theta \sin A \end{pmatrix}.$$

The radiation then travels through a Glan prism positioned at 45° to the polarizer's axis.

The Mueller matrix of this element can be written as

$$M_4 = \frac{1}{2}\begin{pmatrix} 1 & 0 & 1 & 0 \\ 0 & 0 & 0 & 0 \\ 1 & 0 & 1 & 0 \\ 0 & 0 & 0 & 0 \end{pmatrix},$$

and the detector registers radiation with polarization

$$S_4 = M_4 S_3 = \frac{1}{2}\begin{pmatrix} 1 & 0 & 1 & 0 \\ 0 & 0 & 0 & 0 \\ 1 & 0 & 1 & 0 \\ 0 & 0 & 0 & 0 \end{pmatrix}\begin{pmatrix} 1 \\ \cos 2\theta \\ -\sin 2\theta \cos A \\ \sin 2\theta \sin A \end{pmatrix}$$

$$= \frac{1}{2}\begin{pmatrix} 1 - \sin 2\theta \cos A \\ 0 \\ 1 - \sin 2\theta \cos A \\ 0 \end{pmatrix}.$$

The intensity of the detected signal depends on angle of rotation θ and delay A introduced by the photoelastic modulator: $I(t) = \frac{1}{2}[1 - \sin 2\theta \cos A]$.

If the time-dependent change in the delay introduced by modulator is expressed using the Jacobi–Anger expansion, the detected intensity is

$$I(t) = \frac{1}{2}[1 - J_0(A_0)\sin 2\theta + 2J_2(A_0) \times \cos(2\pi 2ft)\sin 2\theta + \dots],$$

where J_0 and J_2 are Bessel functions of the zero and second order, respectively. The first two terms in parentheses are responsible for the constant part of the signal, and the third produces the variable part at the doubled frequency of modulator. We may thus express the constant signal as $V_{dc} = \frac{K}{2[1 - J_0(A_0)\sin 2\theta]}$ and the amplitude of the variable signal as $V_{ac} = V_{2f} = \frac{K}{2}J_2(A_0)\sin(2\theta)$, where K is a proportionality coefficient. Delay A_0 is usually set at 2.405 radians, since the Bessel function of zero order at this value is zero $J_0(A_0 = 2.405) = 0$ and the constant part of the signal V_{dc} becomes insensitive to the rotation of polarization. We can obtain individual amplitudes of the constant and variable parts of the signal by using a signal splitter. Their ratio is proportional to the polarization plane's angle of rotation, $\frac{V_{ac}}{V_{dc}} = \sqrt{2}J_2(A_0 = 2.405)\sin 2\theta$. The angle of rotation is $\theta(\text{rad}) = \frac{1}{2}\arcsin\left[\frac{V_{ac}/V_{dc}}{\sqrt{2}J_2(A_0 = 2.405)}\right]$. Since angle θ is small, approximation $\sin 2\theta \simeq 2\theta$ is valid, and by inserting $J_2(A_0 = 2.405) = 0.4318$ and transforming radians into degrees we can obtain the final expression for the polarization plane's angle of rotation:

$$\theta(\text{degrees}) = 46.91\frac{V_{ac}}{V_{dc}}.$$

This equation ensures an error of less than 1% at angles θ in the range of 0 to 15 degrees. The equation presented above for θ(rad) is used for wide angles.

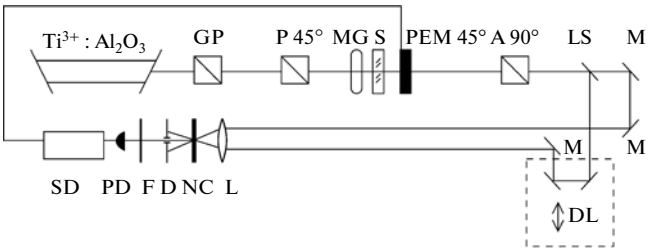

Fig. 2. Scheme of experimental setup of polarization-sensitive autocorrelator for measurement of the time-dynamics of the Faraday effect. GP, Glan prism; P, polarizer; MG, magnet; S, sample; PEM, photoelastic modulator; A, analyzer; LS, light beam splitter; M, mirrors; DL, delay line; L, lens; NC, nonlinear crystal; D, aperture; F, filter; PD, photodiode; SD, lock-in amplifier.

Special methods using, e.g., nonlinear optical effects whose magnitude depends on the intensity of radiation, are required for the detection of femtosecond pulses. The generation of non-collinear second harmonics at the intersection of two light beams is used in the autocorrelation scheme for measuring the duration of femtosecond pulses [17]. The scheme of the experimental setup for measuring the femtosecond dynamics of the Faraday effect is presented in Fig. 2. Let us denote the intensity of the signal transmitted through the fixed mirror system as $I(t)$ and the one transmitted through the delay line as $I(t - \tau)$, where τ is the delay of one signal relative to the other. The intensity of the signal transmitted through the photoelastic modulator is written as $\tilde{I} = I(t)[1 + 4J_2\theta(t)\cos(2\pi 2fT)]$, where T is the characteristic time scale. Hence, the autocorrelation function is expressed as $u(\tau) = \int_{-\infty}^{\infty} \tilde{I}(t)\tilde{I}(t - \tau)dt$,

$$u(\tau) = u_{dc}(\tau)\cos(0) + u_{2f}(\tau)\cos(2\pi 2fT),$$

where $u_{dc}(\tau) = \int_{-\tau/2}^{\tau/2} I(t)I(t - \tau)dt$, $u_{2f}(\tau) = 8J_2\theta(\tau) \times \int_{-\tau/2}^{\tau/2} I(t)I(t - \tau)dt \equiv 8J_2\theta(\tau)u_{dc}(\tau)$; the component proportional to $\theta(\tau)\theta(t - \tau)$ has the second infinitesimal order and can therefore be neglected. We made substitutions $\theta(t) = \theta(\tau)$, $\theta(t - \tau) = \theta(\tau)$, which is valid if the typical time scale of the Faraday rotation

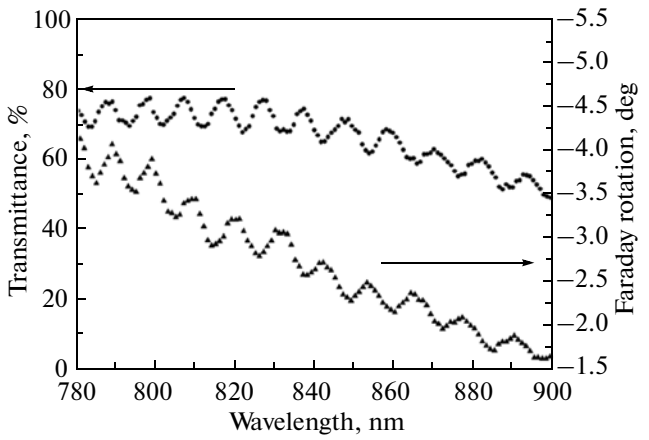

Fig. 3. Optical (dots) and magneto-optical (triangles) spectra of a 16-μm-thick magnetic film.

change is greater than the duration of the pulse transmitted through the delay line. Finally one can write

$$\theta(\tau) \approx \frac{u_{2f}(\tau)}{8J_2 u_{dc}(\tau)}.$$

The value of the Faraday rotation obtained in this manner is averaged over the pulse duration characterizing the change in the polarization plane's angle of rotation, smoothed over the pulse duration.

The polarization-sensitive scheme proposed in [18] was modified to study the Faraday effect dynamics. There are two main parts of the setup: polarization one (located in front of the beam splitter) and correlation one (located behind the beam splitter). Titanium-sapphire laser generating pulses with a central wavelength tunable in the range from 680 to 1080 nm was used as radiation source. The average radiation power changed from 0.9 W at $\lambda = 680$ nm, reached its maximum of 3.5 W at 800 nm, and fell to 0.3 W at 1080 nm in the process. The M^2 parameter of the laser is <1.1, allowing us to consider the shape of the pulse as a TEM00 mode Gaussian. The polarization of the incoming radiation must be linear with an accuracy on the order of the measured rotation angles. Glan prism GP is used to improve the state of polarization. Laser radiation is polarized by the second Glan prism at an angle of 45° (where 0° corresponds to horizontal polarization) and travels through the sample placed in a magnetic field of 1 kOe. It then passes through a photoelastic modulator mounted parallel to the polarizer and rotating the phase of the polarization component with frequency $f = 47$ kHz and delay amplitude 2.405 radians. Finally, it is analyzed using a Glan prism set at an angle of 90°. The polarizer and analyzer are located on rotating stages, allowing them to be rotated with an accuracy of 0.02°. This scheme for the detection of Faraday rotation differs from the one described above, since the radiation reaching the detector is polarized at an angle of 45° in the latter. This configuration of polarizers, however, cannot be used to study ultrafast dynamics because a beam splitter is required for correlation measurements; this introduces changes in the mixed polarization state that are difficult to control and the polarizers are rotated by 45°. As a result, the radiation incident on the splitter has its own state of polarization; it therefore does not change and is transmitted through the subsequent elements of the scheme without distortion.

The radiation is split into two channels using a fifty percent splitter after passing through the Glan prism positioned at 90 degrees. One part passes though a delay line with a minimum step of 80 nm, which corresponds to a time delay of 0.3 fs; the second part travels through a fixed system of mirrors. Parallel beams of the two paths are focused by a collecting lens with a focal length of 50 mm into a single spot on a β-barium borate optical crystal with square nonlinearity. A second harmonic is generated in the crystal in the direction of the angle bisecting the incident beams, and is registered by a detector after passing through a BG39 filter. An aperture blocks the light of the colinear second harmonic from each of the beams, which carry no useful signals. The signal is registered by lock-in detection technique on the doubled frequency of the photoelastic modulator. The dc component of the signal is registered simultaneously. A Hamamatsu H9307-03 photomultiplier is used as a detector.

SAMPLE

The sample is a ferrite–garnet 16-μm-thick film with chemical composition $(Di, Lu, Eu, Tm)_3(Fe, Ga, Al)_5O_{12}$, grown via liquid phase epitaxy on part of a monocrystal $Gd_3Ga_2(GaO_4)_3$ gadolinium–gallium garnet wafer with approximate thickness of ~500 μm. Optical and magneto-optical spectra of the sample are presented in Fig. 3. The transmittance for a given wavelength changes in the range of 40–80%. The contrast between the maximum and the minimum oscillation values in our optical and magneto-optical spectra diminishes as the wavelength grows. There is multiple interference within the film; the thin film acts as a Fabry–Perot interferometer, so transmission spectrum oscilates, and a contrast of oscillation allows us to estimate the field's reflection coefficient. This value was 12% at the film–wafer interface and 40% at the air–film interface. The oscillation period grows from 7 to 12 nm as the wavelength rises. The 800 and 806 nm points in the spectrum were selected for studying the Faraday effect dynamics, since they correspond to the highest contrast between the maximum and minimum stationary values of the Faraday rotation in the period, along with the intermediate value of 803 nm.

RESULTS AND DISCUSSION

Figure 4 presents the initial experimental data—the pulse autocorrelation functions at 0 and 94 kHz frequencies—which were used for retrieving the Faraday

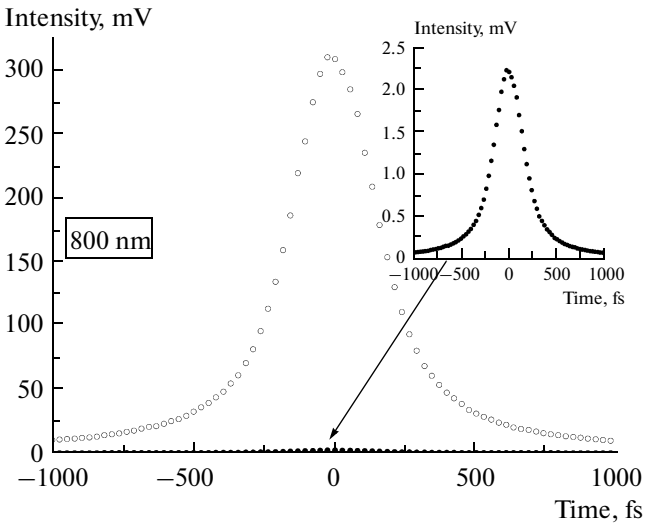

Fig. 4. Autocorrelation functions of laser radiation transmitted through a 16-μm-thick magnetic film at a laser central wavelength of 800 nm. White dots represent the constant signal component; black dots—the alternating component of the signal at doubled modulator frequency.

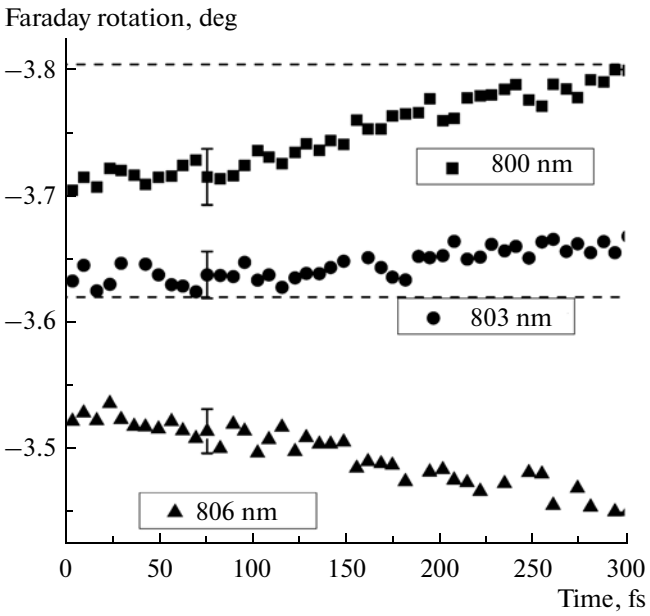

Fig. 5. Time plots of Faraday rotation measured at three wavelengths: 800 nm (squares), 803 nm (circles), and 806 nm (triangles). Steady-state values of the Faraday rotation for 800 and 803 nm.

effect. The ratio of these values for each point in time is proportional to the Faraday rotation. Figure 5 represents the results obtained from our experimental studies of the Faraday effect dynamics in a thin magnetic film at different wavelengths. At a radiation wavelength of 800 nm (squares in Fig. 5), at which the maximal steady-state angle of Faraday rotation is observed, the time plot displays monotonic increase by 0.1° in 300 fs, from −3.7° to almost −3.8°—the steady-state value at this wavelength (dashed line). At the wavelength of 806 nm (triangles in Fig. 5), at which the minimal steady-state angle of Faraday rotation is observed, the dependence monotonically decreases and in the same 300 fs drops by 0.1°, from −3.5° to −3.4°, approaching the steady-state value of −3.2° for this wavelength. When the laser source generates radiation at an intermediate wavelength of 803 nm (circles in Fig. 5), at which the negative derivative of Faraday rotation spectrum is observed, the polarization plane does not rotate in 300 fs and the angle of rotation equals to −3.64°, which agrees with the steady-state value of −3.62° (dashed line) within the limits of experimental error. For the other wavelengths the time dependence increases, decreases or remains constant, depending on whether the Faraday rotation is maximal, minimal, or intermediate at the spectrum. Such behavior of the Faraday rotation can be explained by interference phenomena: pulses are either summing up, enhancing the effect and increasing the Faraday angle of rotation, or canceling each other out and reducing the Faraday rotation, depending on the phase difference between the interfering pulses. There is no evolution of Faraday rotation if the phase difference is $\pi/2$; this corresponds to a situation in which the sample is irradiated by a laser pulse with a wavelength of 803 nm. Hence, phase relation between two interfering pulses determines the particular type of Faraday effect dynamics (increase or decrease); and the latter changes periodically with the spectral shifting of the central wavelength of a pulse.

CONCLUSIONS

Femtosecond dynamics of the Faraday effect in thin magnetic film was studied by polarization-sensitive correlation spectroscopy. Qualitative changes in the time plot of Faraday rotation upon constructive and destructive multiple interference for different spectral positions of the central wavelength of a laser pulse were observed. The measured time dependence of Faraday rotation at a wavelength of 800 nm (the local maximum of the transmittance spectrum) monotonically increases by 0.1°, from −3.7° to −3.8° in 300 fs; for an intermediate wavelength of 803 nm, this dependence is constant of −3.64°; for a wavelength of 806 nm (the local minimum of the transmittance spectrum), the dependence feature monotonic decrease, and the Faraday rotation angle is reduced by 0.1°, from −3.5° to −3.4° within 300 fs. The specific rotation is 6.25×10^{-3} ° μm^{-1} in 300 fs.

ACKNOWLEDGMENTS

This work was supported by the Russian Ministry of Education and Science, and by the Russian Foundation for Basic Research, projects nos. 13-02-01190-a

and 13-02-01336-a. The authors are grateful to A.N. Shaposhnikov, Vernadsky National University of the Crimea, for providing our samples.

REFERENCES

1. Baba, T., *Nature Phot.*, 2008, vol. 2, p. 465.
2. Jorgensen, M.R., Butler, E.S., and Bartl, M.H., *SPIE Proc.*, 2012, vol. 8339, p. 83390Z.
3. Imhof, A., Vos, W.L., Sprik, R., and Lagendijk, A., *Phys. Rev. Lett.*, 1999, vol. 83, p. 2942.
4. Dolgova, T.V., Fedyanin, A.A., Aktsipetrov, O.A., et al., *J. Appl. Phys.*, 2004, vol. 95, p. 11.
5. Inoue, M., Fujii, T., and Abe, M., *J. Appl. Phys.*, 1999, vol. 85, p. 5768.
6. Fedyanin, A.A., Aktsipetrov, O.A., Kobayashi, D., et al., *J. Magn. Magn. Mater.,* 2004, vol. 282, p. 256.
7. Inoue, M., Fujikawa, R., Baryshev, A., et al., *J. Phys. D: Appl. Phys.*, 2006, vol. 39, p. R151.
8. Chung, K.H., Kato, T., Mito, S., et al., *J. Appl. Phys.*, 2010, vol. 107, p. A930.
9. Kimel, A.V., Kirilyuk, A., Usachev, P.A., et al., *Nature,* 2005, vol. 435, p.655.
10. Stanciu, C.D., Hansteen, F., Kimel, A.V., et al., *Phys. Rev. Lett.,* 2007, vol. 99, p. 47601.
11. Bigot, J.Y., Vomir, M., and Beaurepaire, E., *Nat. Phys.*, 2009, vol. 5, p. 515.
12. Kirilyuk, A., Kimel, A.V., and Rasing, T., *Rev. Mod. Phys.*, 2010, vol. 82, p. 2731.
13. Zhang, G.P., Hubner, W., Lefkidis, G., et al., *Nat. Phys.*, 2009, vol. 5, p. 499.
14. Chetvertukhin, A.V., Sharipova, M.I., Zhdanov, A.G., et al., *J. Appl. Phys.*, 2012, vol. 111, p. A944.
15. Hipps, K.W. and Crosby, G.A., *J. Phys. Chem.*, 1979, vol. 83, p. 555.
16. Shercliff, W., *Polarized Light*, Cambridge: Harvard Univ. Press, 1962.
17. Armstrong, J.A., *Appl. Phys. Lett.*, 1967, vol. 10, p. 16.
18. Shcherbakov, M.R., Vabishchevich, P.P., Komarova, V.V., et al., *Phys. Rev. Lett.*, 2012, vol. 108, p. 253903.

Translated by L. Brovko